15 Physics of Biological Systems

Conrad Escher, Hans-Werner Fink, Tatiana Latychevskaia, Jean-Nicolas Longchamp, Marianna Lorenzo, Jonas Verges, Flavio Wicki

in collaboration with: Eugen Ermantraut, Clondiag Chip Technologies GmbH (Germany); Prof. Jannik C. Meyer, University of Vienna (Austria); Prof. Ute Kaiser, University of Ulm (Germany); Prof. Klaus Kern, Max Planck Institut, Stuttgart (Germany); Dr. Yuriy Chushkin and Dr. Federico Zontone, The European Synchrotron Radiation Facility, Grenoble (France); Dr. Annette Niehl and Dr. Manfred Heinlein, CNRS Strasbourg (France), Prof. Christian Schönenberger, University of Basel (Switzerland).

Our primary goal is the structural investigation of individual biological objects, which involves both in-line holography with low energy electrons and coherent diffraction imaging, assisted by micro-structuring techniques using a focused gallium ion beam device for miniaturized electron optics and sample preparation.

Our current activities can be grouped in the following interconnected projects:

- Electron Holography and Coherent Diffraction
  Major experimental challenges are the improvement of the spatial resolution, the creation of free standing films of graphene transparent for low-energy electrons and the presentation of a single protein molecule to a coherent electron wave front. Another, equally important aspect for achieving high resolution structural information is the optimal hologram reconstruction, developing numerical algorithms to solve the integrals governing these coherent optics problems.

- Coherent Diffraction Imaging of Graphene-Supported Single Biomolecules at Atomic Resolution
  This is an independent effort (Ambizione project) of Jean-Nicolas Longchamp. Methods to deposit biomolecules onto freestanding graphene, in particular in-situ electrospray deposition, have been explored. The successful imaging of biomolecules was cross-validated by TEM investigations at the microscopy center of our University. First detailed studies of a single virus are described in some detail below.

- Electron and Ion Point Sources
  Field Ion Microscopy and related techniques are employed for fabricating and using bright electron and ion point sources. A novel bright proton source has recently been developed and used for Proton Projection Microscopy which complements imaging with coherent electrons within the very same system.

- Resolution enhancement in X-ray coherent diffraction imaging by extrapolation of diffraction patterns
  In collaboration with a group at the European Synchrotron Radiation Facility in Grenoble, we have enhanced the resolution of a non-crystalline object obtained from an X-ray diffraction pattern by extrapolation beyond the detector area. The primary record is missing about 10% information, including the pixels in the center of the diffraction pattern. The extrapolation is based on an iterative routine. A joint publication is currently under review.

15.1 Instrumentation

A new Low Energy Electron Point Source (LEEPS) microscope has been designed (Fig. 15.1) and built (Fig. 15.2) by our machine shop. The ultra-high vacuum compatible instrument is expected to be in operation by summer 2015.

We have been combining LEEPS microscopy with the functionality of STM for the study of freestanding atomically thin films and objects deposited onto them. These techniques require similar hardware instrumentation but

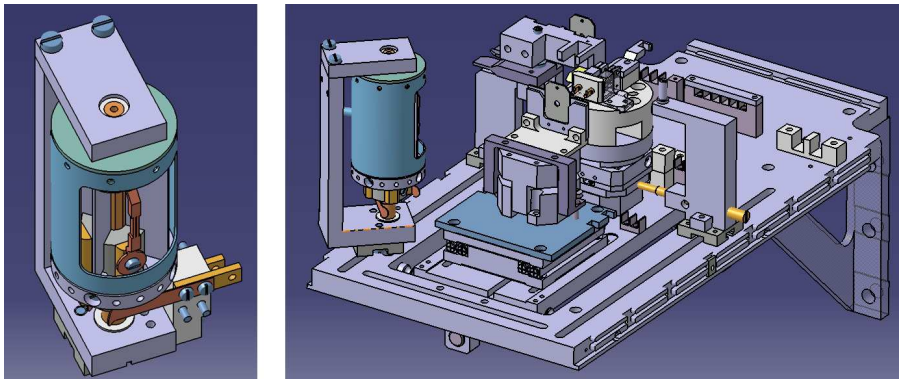

FIG. 15.1 – Overall design of a new LEEPS microscope for exploring in situ adsorption of alkali atoms onto freestanding graphene. Up to four alkali metals can be evaporated. The rotatable evaporator is shown in more detail on the left.

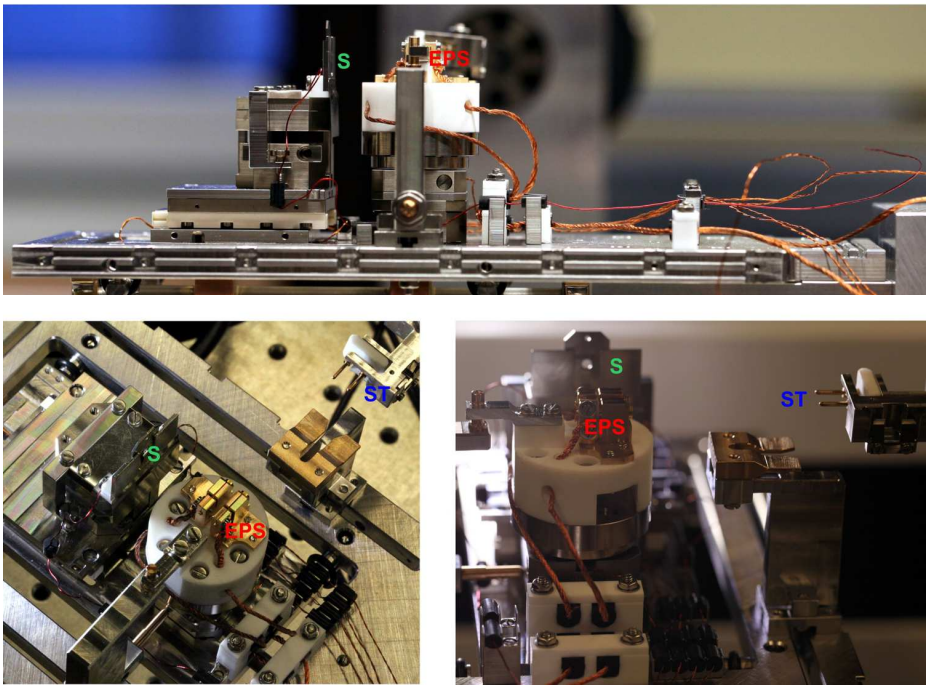

FIG. 15.2 – Status of the new LEEPS system as of March 2015.
EPS: electron point source;
S: sample and
ST: transfer mechanism which allows to move samples and tips (electron point sources) without braking the ultra-high vacuum.

offer different, complementary imaging properties. The most crucial modification to our previous system is the implementation of STM electronics and a software package dedicated to STM signal and data processing.

For our recent review of the subject, see:
Holography and coherent diffraction with low-energy electrons: A route towards structural biology at the single molecule level, `www.sciencedirect.com/science/article/pii/S030439911400240X`.

15.2 Imaging tobacco mosaic virus by low-energy electron holography

Jean-Nicolas Longchamp, Tatiana Latychevskaia, Conrad Escher and Hans-Werner Fink

Structural information about biomolecules at nanometer, sub-nanometer or atomic resolution is nowadays predominantly obtained by X-ray crystallography and NMR spectroscopy, whereby samples in the form of crystals or in liquids are studied. This, however, entails important structural information being averaged over many molecules. Thus, relevant details in molecules exhibiting diverse structural conformations remain undiscovered. Besides this drawback, these methods can only be applied to a limited subset of biological molecules that either readily crystallize for use in X-ray studies or are small enough for NMR investigations. A third approach towards imaging single particles is cryo-electron microscopy; however, for biological samples the possible resolution is limited by radiation damage caused by the high electron energy employed in conventional transmission electron microscopes (TEM) [1]. Due to the strong inelastic scattering of high-energy electrons, there is little hope for obtaining structural information at atomic resolution for a single entity. As the permissible dose is limited to 10 e-/ Å^2 only, an individual molecule is destroyed long before an image of high enough quality could be acquired [2, 3]. The radiation damage problem is usually circumvented by averaging over several thousand noisy images in order to attain a satisfactory signal-to-noise ratio [4]. The alignment and averaging routines inherent to high-resolution cryo-electron microscopy limit its application range to symmetric and particularly rigid objects, such as specific classes of viruses.

Despite the shortcomings of the three conventional structural biology tools discussed above, one needs to express respect for the vast amount of data that has been generated over the past decades, reflected by the impressive volume of the current protein database [5]. Nevertheless, a milestone for structural biology would definitely be attained if methods and tools were available, that do away with averaging over an ensemble of molecules and enable structural biology on a truly single molecule level. To obtain atomic resolution information about the structure of any individual biological molecule, different concepts and technologies are needed. One approach of this kind is associated with the recent X-ray free electron laser (XFEL) projects. This approach initially appeared to be a promising method for gaining information from just one single biomolecule at the atomic scale by recording its X-ray diffraction pattern within the short time of just 10 fs, before the molecule is decomposed by radiation damage. Unfortunately, there are now strong indications [6] that again averaging over a large number of molecules is in-

evitable in order to obtain images with a sufficiently high signal-to-noise ratio enabling numerical reconstruction of the diffraction pattern with atomic resolution [7–9].

The approach to structural biology at the single molecule level described here, is motivated by the experimental evidence that electrons with a kinetic energy in the range of 50 - 250 eV are harmless to biomolecules [10–12]. Even after exposing fragile molecules like DNA or proteins to a total electron dose of 10^6 e-/Å^2, i.e. more than five orders of magnitude higher than the critical dose in TEM, no radiation damage could be observed. This, combined with the fact that the de Broglie wavelengths associated with this energy range are between 0.7 and 1.7 Å, makes low-energy electron microscopy an auspicious candidate for structural biology at the single molecule level.

During the last three decades, DNA, phages, viruses and individual ferritin proteins attached to carbon nanotubes were imaged by means of low-energy electron holography with nanometer resolution [10, 11, 13–15]. For imaging, the objects of interest used to be placed across bores in a membrane. Unfortunately, after such preparation the holographic record often suffered from biprism distortion limiting the resolution in the reconstruction [16]. This artifact is suppressed if the specimen is placed on an electrically conductive substrate with sufficient transparency for low-energy electrons [17, 18]. Yet, the substrate has to be robust enough to withstand the deposition procedure [19]. It turned out that freestanding graphene, an atomically thin layer of carbon atoms arranged in a honeycomb lattice, fulfills all these requirements. Electron transmission measurements have shown that more than 70% of the low-energy electrons are transmitted through graphene and therefore are available for imaging objects deposited on the two dimensional substrate [17].

The discovery of the tobacco mosaic virus (TMV) at the end of the 19th century marked the beginning of what is now called virology [20–22]. Starting from 1936, TMV was the object of several X-ray diffraction investigations. In that year, Bawden *et al.* could retrieve a repeating pattern with a periodicity of 2.2 nm, a measure nowadays associated with the pitch of the helical TMV structure [23]. Only three years later, Kausche, Pfankuchn and Ruska were able to image TMV in an early version of a TEM [24]. In this pioneer work they disclosed the rod-like shape of the virus with dimensions of 300 nm in length and 15 nm in width. These findings are still in good agreement with the current values of 300 nm and 18 nm, respectively. Based on the data available at the time, Watson and Franklin proposed the helical TMV structure in 1954 and 1955, respectively [23]. The first molecular model at atomic resolution was obtained from X-ray fiber diffraction experiments by Namba et al. in 1986 [25, 26].

Retrieving information about unstained TMV at the sub-nanometer scale is possible by means of cryo-electron microscopy since the 1980's [27, 28]. The most recent models that can be found in the protein database are either obtained from X-ray fiber diffraction data (2.9Å resolution) or transmission electron microscopy investigations (5 Å resolution) [5]. In both cases, the Angstrom resolution could only be obtained by averaging over a vast number of entities.

We shall show below that by means of low-energy electron holography, it is possible to image individual TMVs deposited on ultra-clean freestanding graphene. The viruses are imaged with one nanometer resolution exhibiting details of the helical TMV structure.

15.2.1 Materials and Methods

In our low-energy electron holographic setup, inspired by Gabor's original idea of in-line holography [29–31], a sharp (111)-oriented tungsten tip acts as source for a divergent beam of highly coherent electrons [31–34]. The electron emitter can be brought as close as 100 nm to the sample with the help of a 3-axis nano-positioner. The part of the electron wave elastically scattered off the object is called the object wave, while the un-scattered part represents the reference wave. At a distant detector, the resulting interference pattern, the hologram, is recorded. The magnification of the imaging system, given by the ratio between detector-to-source and sample-to-source distances, can be up to hundred.

A hologram, in contrast to a diffraction pattern, contains the phase information of the object wave, and the

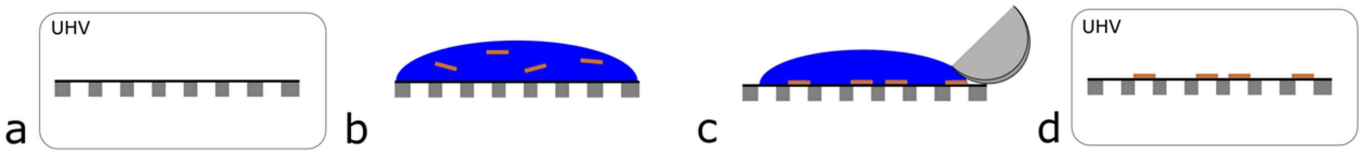

FIG. 15.3 – Virus deposition on ultra-clean freestanding graphene. (a) The cleanliness of the graphene sample carrier is first inspected by means of low-energy electron holography under UHV conditions; (b) A 0.5 ng/μl drop of TMV solution is applied onto the substrate; (c) After waiting a few seconds for the sedimentation of the viruses, the excess water is removed with blotting paper and (d) The sample is heated to 125°C for 45 min.
The viruses are now ready to be imaged by means of low-energy electron holography.

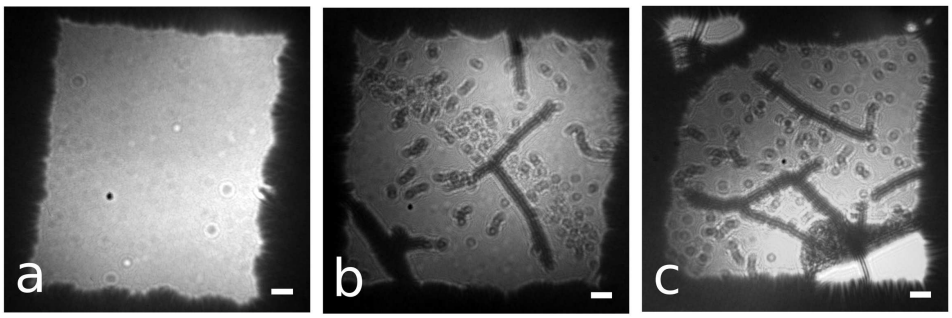

FIG. 15.4 – (a) Low-energy electron hologram of freestanding graphene covering a square aperture milled in a Pd-coated SiN membrane. The graphene layer appears ultra-clean. (b) and (c): Holograms of after TMV deposition. Scale bars correspond to 50 nm.

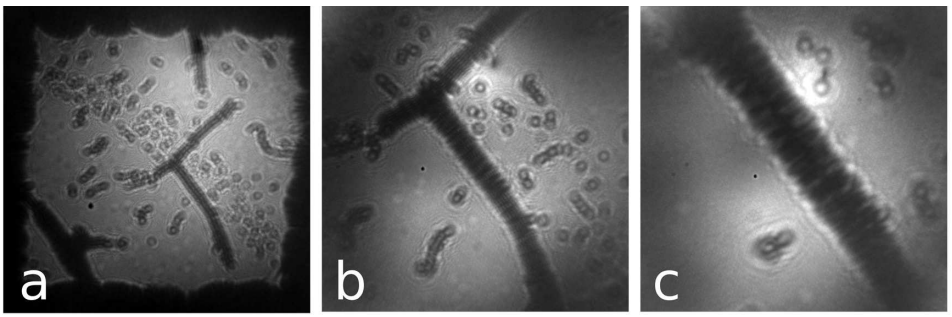

FIG. 15.5 – Low-energy electron holograms with increasing magnification and decreasing source-to-sample distance. The electron energy amounts to 131 eV in (a), 103 eV in (b) and 89 eV in (c) and the source-to-sample distances to 1500 nm, 450 nm and 180 nm, respectively.

object structure can thus be reconstructed unambiguously. The reconstruction is achieved by back propagation of the hologram, which corresponds to a Fresnel-Kirchhoff integral transformation [35–39]. The resolution is limited by the de Broglie wavelength (λ) and the numerical aperture of the detector (NA). With $\lambda = 0.7$ Å and NA = 0.54, atomic resolution shall be possible.

Ultra-clean freestanding graphene, covering ion milled square-like apertures of approximately 500 nm side length, is prepared by the platinum-metal catalysis method [40]. Thereafter, the cleanliness of the graphene is inspected in our low-energy electron holography microscope operating under UHV conditions. Viruses were prepared following the recipe by Niehl *et al.* [41]. They were extracted from ORMV-infected nicotiana benthamiana leaves, purified by precipitation and sedimentation and re-suspended in 10 mM sodium-phosphate buffer. For TMV deposition (see Fig. 15.3), graphene samples prepared as described above are taken out of the low-energy electron microscope.

15.2.2 Results and Discussion

Figure 15.4 displays low-energy electron holograms recorded at kinetic energies of 131 eV and 125 eV. In these images, the rod-like viruses are apparent besides traces of dirt resulting from the sample preparation procedure.

In contrast to TEM, in low-energy electron holography no lenses are employed and the magnification power of the instrument can be chosen simply by changing the distance between electron source and sample. If the field emission current is maintained constant, the reduction of the source-to-sample distance implies also a decrease of the electron energy (see Fig. 15.5). With increasing magnification, the interference fringes become more and more pronounced.

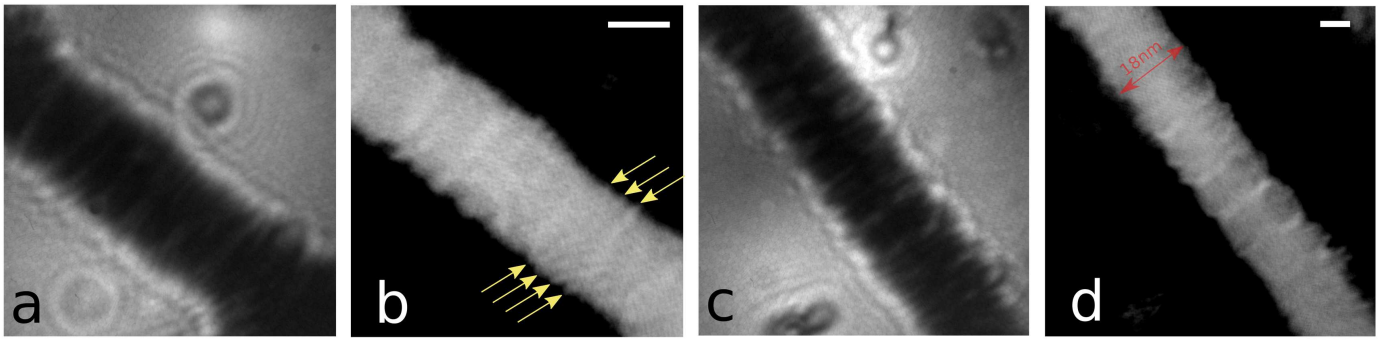

FIG. 15.6 – High-magnification holograms of TMV and the respective reconstructions. (a) and (c) Holograms of TMV recorded with 80 eV, respectively 89 eV electron energy. (b) and (d) reconstructed TMV images from (b) and (c) (inverted grayscale). Arrows emphasize the presence of apex-like features on the rim of the TMV. These details are attributed to the helical structure of the virus. The scale bare corresponds to 10 nm.

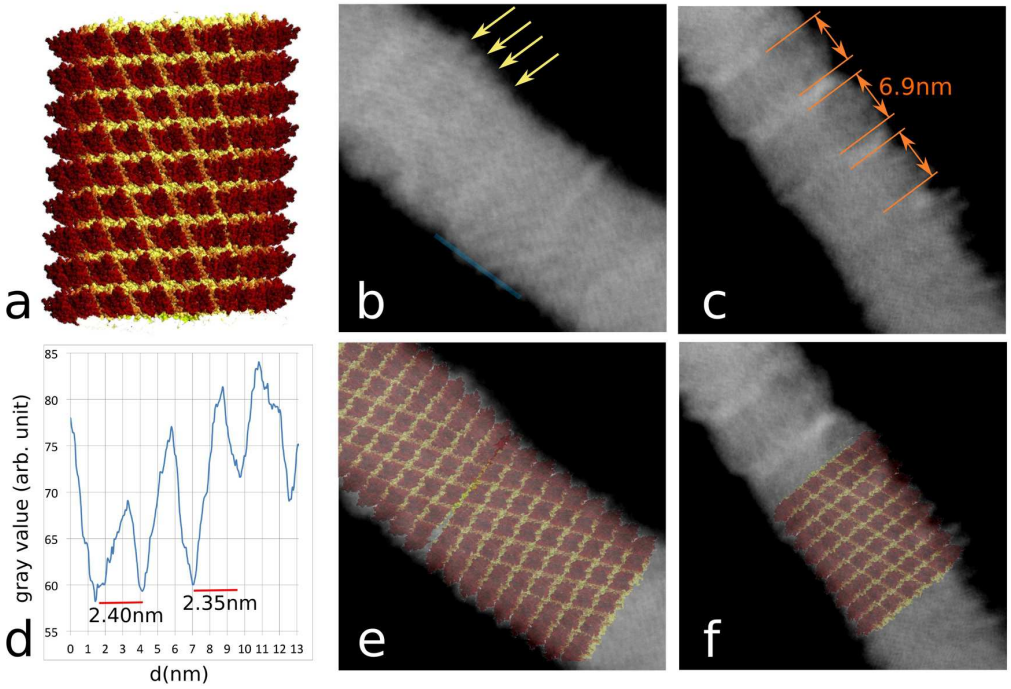

FIG. 15.7 – Confronting an atomic TMV model with the measurements.
(a) Atomic TMV model constructed from the available coordinates [42].
(b)-(c) Close-ups of the images in Fig. 15.6.
(d) Intensity scan along the blue line in (b).
(e)-(f) Images as in (b)-(c) with the atomic TMV model superimposed.
In (b) arrows mark further apex-like features coinciding with the atomic model. In (c) the distance between bright stripes is marked according to the literature value of 6.9 nm for the thickness of a subunit.

In Figs. 15.6a and 15.6c, two high magnification holograms are displayed. From these holograms the shape of the corresponding viruses is reconstructed at one nanometer resolution (see Figs. 15.6b and 15.6d). The diameter of the virus corresponds to 18 nm as expected. Furthermore, one can observe, as emphasized by arrows in Fig. 15.6b, apex-like features on the rim of the virus, which we attribute to the helical TMV structure.

Given an electron de-Broglie wavelength around 1.4 Å and since in low-energy electron holography the resolution is neither limited by lens aberrations nor by radiation damage, Angstrom resolution may be expected. The nanometer resolution that we report here is attributed to residual mechanical vibrations. In a low-energy electron hologram the spacing between consecutive interference fringes gradually decreases towards higher orders. Hence, high-order interference fringes and thus finest structural details are most susceptible to such vibrations.

Even if the current resolution is of the order of one nanometer, one can already compare the images obtained with low-energy electrons with an atomic TMV model constructed by Jean-Yves Sgro [42] with the atomic coordinates available from the protein database (Fig. 15.7a). Figures 15.7b and 15.7c are close-ups of the TMV images displayed in Fig. 15.6. Once the atomic TMV model is superimposed to match the width of the viruses (see Figs. 15.7e and 15.7f), the apex-like features that we previously attributed to the helical structure of the virus are now coinciding with the peaks of the helical structure in the model.

The agreement between model and experimental data obtained from a single particle is remarkable. To take into account the kink in the TMV shown in Fig. 15.7e, two copies of the model, rotated by 6° with respect to each other, are superimposed on the low-energy electron images. By this, further details, marked by arrows in Fig. 15.7b, which correspond to the helical structure ofthe virus are now congruent with the atomic model. In Fig. 15.7d, an intensity plot along the blue line present in Fig. 15.6b is displayed. The distance between depletions in this graph corresponds to approximately 2.35-2.40 nm, a length that almost perfectly fits the expected 2.30 nm helical pitch from X-ray fiber diffraction investigations [5, 43, 44]. Moreover, in Fig. 15.7b-c equidistant bright stripes across the virus are visible. The distance between these features amounts to approximately 7 nm, which most likely corresponds to the literature value of 6.9 nm associated with the thickness of a TMV subunit [44, 45]. Such stripes have been observed in TEM investigations of uranyl acetate stained in-vitro assembled viruses [46, 47] but, to our knowledge, never on in-vivo purified TMV.

With this, we have demonstrated the potential of low-energy electron holography for structural biology at the single particle level. The mapping of any internal structure of the virus is precluded due to the thickness of TMV. However, this limitation is only relevant for objects thicker than 5 nm, i.e. thicker than the majority of proteins for instance.

The current nm resolution will soon be pushed to Å resolution by improving the mechanical stability. Furthermore, we have recently reported that by employing a slightly modified experimental setup, where a parallel

beam of low-energy electrons is illuminating the sample, we could image a region of 210 nm in diameter of freestanding graphene with 2 Å resolution [48]. This scheme will be used to image TMV with a similar resolution.

The sample preparation method used here is certainly only applicable for a very small subset of biological entities that withstand the heat treatment. However, we have recently shown that it is possible to electrospray deposit *in vacuo* gold nanorods of 20 MDa molecular weight onto freestanding graphene without damaging the atomically thin substrate [12]. This demonstrates that the deposition of proteins onto graphene is within reach and consequently structural biology at the single particle level by means of coherent low-energy electron microscopy should soon emerge.

15.2.3 Acknowledgements

We would like to thank Annette Niehl and Manfred Heinlein from the CNRS Strasbourg for the TMV purification and helpful discussions. We also thank Kishan Todkar and Christian Schönenberger from the University of Basel for providing us with their CVD grown graphene.

[1] R. Henderson, Rev. Biophys. 28(2) (1995) 171.
[2] R.F. Egerton, P. Li, M. Malac, Micron 35(6) (2004) 399.
[3] E. Knapek, J. Dubochet, J. Mol. Biol. 141(2) (1980) 147.
[4] M. van Heel, *et al.*, Q. Rev. Biophys 33(4) (2000) 307.
[5] Protein Data Bank, *www.pdb.org*.
[6] J.W. Miao, *et al.*, Annu. Rev. Biophys. Biomol. Struct. 33 (2004) 157.
[7] R. Neutze, *et al.*, Nature 406(6797) (2000) 752.
[8] V.L. Shneerson, *et al.*, Acta Crystallogr. Sect. A 64 (2008) 303.
[9] H.N. Chapman, *et al.*, Nature 470(7332) (2011) 73.
[10] M. Germann, T. Latychevskaia, C. Escher, H.-W. Fink, Phys. Rev. Lett. 104(9) (2010) 95501.
[11] J.-N. Longchamp, T. Latychevskaia, C. Escher, H.-W. Fink, Appl. Phys. Lett. 101(9) (2012) 93701.
[12] T. Latychevskaia, Longchamp J-N, C. Escher, H.-W. Fink (2014) Ultramicroscopy.
[13] H.-W. Fink, H. Schmid, E. Ermantraut, T. Schulz, J. Opt. Soc. Am. A - Opt. Image. Sci. Vis. 14(9) (1997) 2168.
[14] G.B. Stevens, *et al.*, Eur. Biophys. J. 40 (2011) 1197.
[15] P. Simon, *et al.*, Micron 39(3) (2008) 229.
[16] T. Latychevskaia, J.-N. Longchamp, C. Escher, H.-W. Fink, Ultramicroscopy 145 (2014) 22.
[17] J.-N. Longchamp, T. Latychevskaia, C. Escher, H.-W. Fink, Appl. Phys. Lett. 101(11) (2012) 113117.
[18] J.-N. Longchamp, C. Escher, T. Latychevskaia, H.-W. Fink, Ultramicroscopy (2014).
[19] R.R. Nair, *et al.*, Appl. Phys. Lett. 97(15) (2010) 153102.
[20] D. Ivanowski, St Petersb. Acad. Imp. Sci. Bul. (1892).
[21] M.W. Beijerinck, *Over een Contagium vivum fluidum als oorzaak van de vlekziekte der tabaksbladeren*, Koninkl. Akademie van Wetenschappen (1898) 229.
[22] E.F. Smith, J. Mycol. 7(4) (1894) 382.
[23] J.D. Watson, Biochim. Biophys. Acta 13 (1954) 10.
[24] G.A. Kausche, *et al.*, Naturwissenschaften 27 (1939) 292.
[25] K. Namba, G. Stubbs, Science 231(4744) (1986) 1401.
[26] K. Namba, *et al.*, J. Mol. Biol. 208(2) (1989) 307.
[27] T.-W. Jeng, *et al.*, J. Mol. Biol. 205(1) (1989) 251.
[28] C. Sachse, *et al.*, J. Mol. Biol. 371(3) (2007) 812.
[29] D. Gabor, Nature 161(4098) (1948) 777.
[30] D. Gabor, *Holography*, Nobel Lect. (1971).
[31] H.-W. Fink, W. Stocker, H. Schmid, Phys. Rev. Lett. 65(10) (1990) 1204.
[32] H.-W. Fink, Ultramicroscopy 50(1) (1993) 101.
[33] H.-W. Fink, IBM J. Res. Dev. 30(5) (1986) 460.
[34] H.-W. Fink, W. Stocker, H. Schmid, J. Vac. Sci. Technol. B 8(6) (1990) 1323.
[35] H.J. Kreuzer, *et al.*, Ultramicroscopy 45(3-4) (1992) 381.
[36] H.J. Kreuzer, Micron 26(6) (1995) 503.
[37] T. Latychevskaia, H.-W. Fink, Phys. Rev. Lett. 98(23) (2007) 233901.
[38] T. Latychevskaia, H.-W. Fink, Opt. Express 17(13) (2009) 10697.
[39] T. Latychevskaia, J.-N. Longchamp, H.-W. Fink, Opt. Express 20(27) (2012) 28871.
[40] J.-N. Longchamp, C. Escher, H.-W. Fink, J. Vac. Sci. Technol. B Microelectron Nanom. Struct. 31(2) (2013) 020605.
[41] A. Niehl, *et al.*, Plant Physiol. 160(4) (2012) 2093.
[42] C.M Fauquet, *et al.*, eds. (2005) Virus Taxonomy: VIIIth Report of the International Committee on Taxonomy of Viruses (Academic Press London and New York).
[43] F. Bawden, *et al.*, Nature 138 (1936) 1051.
[44] R.E. Franklin, Biochim. Biophys. Acta 19 (1956) 203.
[45] A. Kendall, *et al.*, Virology 369(1) 226.
[46] A.C.H. Durham, *et al.*, Nature 229(2) (1971) (2007) 37.
[47] P.J. Butler, Philos. Trans. R. Soc. Lond. B, Biol. Sci. 354(1383) (1999) 537.
[48] J.-N. Longchamp, T. Latychevskaia, C. Escher, H.-W. Fink, Phys. Rev. Lett. 110(25) (2013) 255501.